VOL. 12 NO. 9,
MAY, 2026
E-ISSN 3026-958X
P-ISSN 3027-1169

African Scholar Publications & Research International
www.africanscholarpub.com

Journal of Science Innovation & Technology Research (JSITR)

Box-Behnken Design Approach to Optimize the Extraction and Characterization of Neem (*Azadirachta indica*) Seed Oil

J. E. Sinebe[1]; E. T. Erokare[2]; & W. C. Ulakpa[3]

[1]Department of Mechanical Engineering, Delta State University, Abraka, Nigeria.
[2]Department of Agricultural and Biosystem Engineering, Southern Delta University, Ozoro, Nigeria. [3]Department of Chemical Engineering, Southern Delta University, Ozoro, Nigeria.

Corresponding Author: erokaretega.e@gmail.com

DOI: https://doi.org/10.70382/ajsitr.v12i9.086

Abstract

This study introduces a novel and efficient optimization strategy for the solvent extraction of neem (Azadirachta indica) seed oil, a promising non-edible feedstock for biodiesel production, using a three-factor Box-Behnken Design (BBD) under Response Surface Methodology (RSM). The innovation lies in the systematic integration of statistical modeling with conventional Soxhlet extraction using n-hexane, focusing on the interactive effects of reaction temperature (50–80 °C), extraction time (40–60 min), and particle size (0.14–0.20 mm). A highly significant quadratic model (F-value = 21.21, p = 0.0003, R^2 = 0.9646) was developed, revealing temperature as the dominant linear factor and strong quadratic effects for all variables. The optimized conditions yielded a maximum oil extraction of 39.93% (predicted), closely validated by confirmatory experiments (relative error < 2.5%). The extracted oil exhibited a high acid value (172 mg KOH/g), confirming its suitability as a low-cost, non-edible biodiesel precursor after acid pre-treatment, while FTIR analysis verified the presence of characteristic triglyceride functional groups. This work represents a significant advancement by providing a scalable, cost-effective, and statistically robust protocol for valorizing abundant neem seeds in resource-limited settings. It bridges the gap between conventional extraction techniques and modern optimization tools, offering a replicable model for enhancing oil yield while supporting sustainable biofuel development.

Keywords: Azadirachta Indica, Neem Oil, Response Surface Methodology, Box-Behnken Design, Process Optimization, Solvent Extraction.

Introduction

The neem tree (Azadirachta indica A. Juss.), a member of the Meliaceae family, is widely acknowledged as a versatile multipurpose plant with significant economic, medicinal, and industrial value. Native to the Indian subcontinent and extensively cultivated in tropical and subtropical regions worldwide, including parts of Africa, the tree produces seeds that are rich in oil, typically ranging between 30% and 50% by weight depending on variety, environmental conditions, and processing methods. Neem seed oil (NSO) is a complex mixture of triglycerides and numerous bioactive compounds, notably limonoids such as azadirachtin, nimbin, and nimbidin, which confer potent insecticidal, antimicrobial, antifungal, and antioxidant properties (Suttiarporn & Choommongkol, 2020).

Beyond its traditional applications in medicine, cosmetics, and biopesticides, neem seed oil has gained increasing attention as a promising non-edible feedstock for biodiesel production. Its high oil content and favorable fatty acid profile, dominated by oleic and linoleic acids, make it a sustainable alternative to edible oils, thereby avoiding competition with food resources. However, the efficiency of oil extraction significantly influences both the yield and the quality of the final product, particularly the preservation of thermolabile bioactive constituents (Ameen et al., 2023).

Conventional solvent extraction using n-hexane remains one of the most widely employed industrial methods for recovering neem seed oil due to its relatively high efficiency and scalability. Nevertheless, the process is affected by multiple interacting parameters, including extraction temperature, time, particle size of the seed meal, and solvent-to-solid ratio. Traditional one-factor-at-a-time optimization approaches often fail to capture these complex interactions, leading to suboptimal yields and increased energy consumption (Nde & Foncha, 2020).

In recent years, Response Surface Methodology (RSM) has emerged as a powerful statistical tool for process optimization in oil extraction studies. Among various RSM designs, the Box-Behnken Design (BBD) is particularly advantageous for three-factor experiments as it requires fewer runs, efficiently estimates quadratic and interaction effects, and avoids extreme experimental points that could degrade heat-sensitive compounds (Amin et al., 2026).

Previous studies on neem seed oil extraction have utilized various techniques. For instance, several researchers applied RSM with Central Composite Design (CCD) for ultrasonic-assisted extraction, achieving higher yields but at the cost of higher energy input (e.g., studies reporting 35–45% yields with sonication). Microwave-assisted methods have also been explored, offering reduced extraction times (20–40 min) while preserving bioactive compounds. Supercritical fluid extraction with CO_2 has demonstrated superior quality oil but faces

scalability challenges due to high equipment costs. In contrast, the present solvent-based BBD optimization focuses on conventional Soxhlet scalability, lower operational costs, and systematic evaluation of temperature, time, and particle size interactions, thereby complementing these advanced methods for industrial applicability in resource-limited settings (Martínez-Castro et al., 2024).

This study employs a Box-Behnken Design approach to systematically optimize the solvent extraction of neem seed oil, followed by comprehensive physicochemical characterization of the extracted oil. The research aims to establish optimal operating conditions that maximize oil yield while maintaining desirable quality attributes suitable for industrial applications, particularly biodiesel production. By integrating statistical modeling with detailed oil characterization, this work contributes to the sustainable valorization of neem seeds as a renewable resource in the oleochemical and biofuel sectors (Kazam etal., 2025).

Materials and Methods

The raw neem seeds, collected from Suleja and Bida in Niger State, were prepared by repeated washing and oven-drying at 60 °C for 24 hours to standardize their moisture content. A laboratory mill was used to reduce the dried seeds to a powder. Analytical grade reagents for the extraction were sourced from Palmlac Chemical Products (Minna, Niger State). The overall sequence of the oil extraction process is detailed in the flow chart presented in Figure 1.

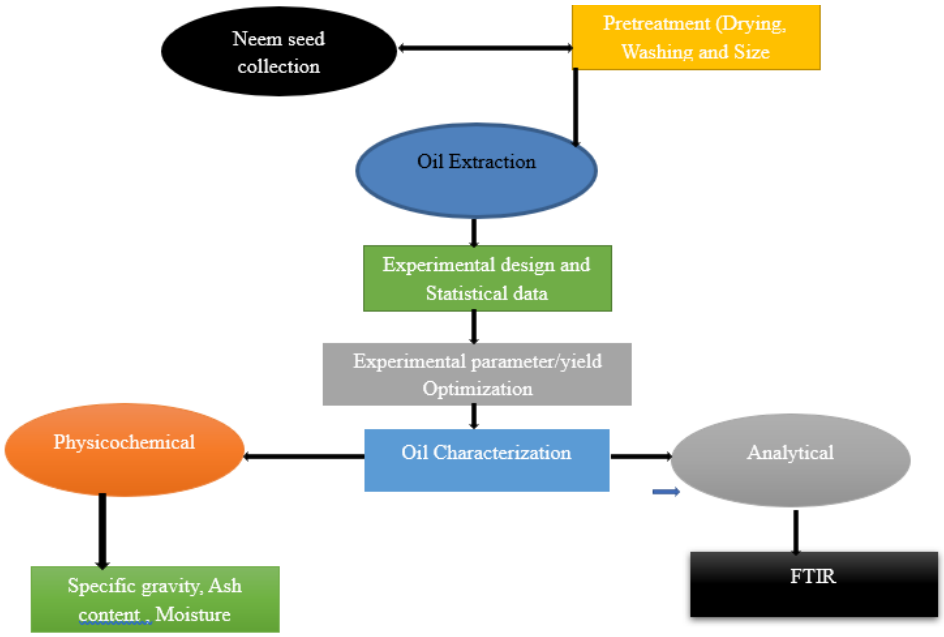


Figure 1. Neem Seed oil Extraction Process Flow Chart

Solvent Extraction Procedure

The Soxhlet extraction was carried out using a standard laboratory Soxhlet apparatus (250 mL flask, condenser, thimble). The heating mantle temperature was controlled at set points corresponding to the coded levels of the design (ranging from approximately 50 to 80 °C as measured on the mantle controller).

Extractions used a solvent-to-solid ratio of 10:1 (mL/g) with 10 g of dry kernel powder per run. The Soxhlet apparatus operated with approximately 4–6 reflux cycles per minute at optimal conditions. The heating mantle temperature was calibrated using a digital thermometer inserted in the mantle controller to ensure accurate set points. Neem seed oil was extracted using a standard laboratory Soxhlet apparatus consisting of a 250 mL round-bottom flask, a 30 mm × 100 mm cellulose extraction thimble (Whatman or equivalent), and a water-cooled Allihn condenser.

The actual temperature inside the thimble was close to the boiling point of n-hexane (69 °C at atmospheric pressure) during active reflux. The variable labeled 'extraction temperature' in the experimental design therefore primarily influenced the reflux rate and cycle frequency rather than the sample temperature itself.

All extractions were conducted at atmospheric pressure. No pressurized system or condenser temperature manipulation was employed. Temperature was measured using the heating mantle digital controller (not inside the thimble). The actual temperature experienced by the sample during solvent contact was therefore approximately constant at the boiling point of n-hexane

Oil yield (%) was calculated on a dry kernel basis as follows:

The extraction yield was calculated using Equation (1).

$$Oil\ Yield\ (\%) = \frac{\dot{mass\ of\ extracted\ oil}}{dry\ mass\ of\ neemseed\ kernel\ powder} \times 100 \qquad (1)$$

To establish the maximum extractable oil content, exhaustive extraction was performed on the same kernel powder using n-hexane in a Soxhlet apparatus for 24 hours (multiple solvent cycles until no additional oil was extracted). This served as a benchmark for the true oil content of the material.

The optimization of oil extraction parameters was conducted using a Box-Behnken experimental design. This design incorporated three independent variables: heating mantle temperature (50–80 °C, corresponding to varying reflux rates; actual sample temperature 69 °C) , extraction time (40–60 minutes), and particle size (0.14–0.2 mm), as outlined in Table 1. A total of 17 experimental runs, including replicates, were performed (Table 1).

The resulting data were analyzed using the Box-Behnken model framework. A multiple regression approach was applied to fit the experimental results to a model Equation. (2), evaluating linear, interactive, and quadratic effects of the parameters on the extraction yield.

$$Y = \beta_0 + \Sigma\beta_i X_i + \Sigma\beta_{ii} X_i^2 + \Sigma\beta_{ij} X_i X_j + \varepsilon \qquad (2)$$

Where: Y is the predicted response, β_0 is the constant/intercept term, β_i are the linear coefficients, β_{ii} are the quadratic coefficients, β_{ij} are the interaction coefficients, X_i and X_j represent the independent variables, ε is the random error.

Table 1. Box-Behnken Design Parameters for Neem Seed Oil Extraction

Factor	Name	Units	Coded Low	Mean	Coded High
A	Reaction temperature	^{O}C	50.00	65.00	80.00
B	Reaction time	min	40.00	50.00	60.00
C	Particle size	mm	0.14	0.1700	0.20

Physicochemical Properties/analytical Properties of Neem Seed Oil

The quality, stability, and commercial value of neem seed oil are determined by its physicochemical properties. These properties are routinely evaluated using standardized methods, many of which are established by the AOAC and American Society of Testing Material (ASTM). Fatty Acids (FFA), Peroxide Value (PV), Saponification Value (SV), Iodine Value (IV), Peroxide Value (PV), Moisture and Volatile Matter Content, Specific Gravity, and Fourier transform infrared spectrometer. The following are the critical quality parameters for neem seed oil: Acid Value (AV) and Free.

Results and Discussion

Experimental Design and Statistical Data Analysis

Analysis of variance (ANOVA) is a key statistical technique used to assess the overall significance and adequacy of the developed quadratic model. As shown in Table 3, the model F-value of 21.21 with a corresponding p-value of 0.0003 indicates that the model is highly significant. This means there is only a 0.03% chance that the observed relationship between the process variables (temperature, time, and particle size) and oil yield could have occurred due to random experimental noise. In other words, the model reliably captures the true effects of the independent variables on the extraction process.

The lack-of-fit test further supports model adequacy, yielding an F-value of 0.2836 and a p-value of 0.8357 (not significant). This suggests that the variation due to pure error from replicate center points exceeds any lack of fit, confirming that the quadratic model adequately fits the experimental data (Wisdom et al., 2022).

The coefficient of determination (R^2) of 0.9646 shows that the model explains 96.46% of the total variability in neem seed oil yield, indicating a very good fit. The adjusted R^2 value of 0.9191 remains high and in reasonable agreement with R^2, demonstrating that the model is not over-parameterized. Moreover, the predicted R^2 of 0.8552 reveals strong predictive power, meaning the model can reliably estimate oil yields for new conditions within the studied design space. The adequate precision ratio of 13.101 (well above the desirable threshold of 4)

confirms an adequate signal-to-noise ratio, making the model suitable for navigating the design space and optimization.

Examination of the coefficient estimates in Table 4 provides deeper insight into the contribution of each factor. Reaction temperature exhibited a large positive linear coefficient (+4.11) with high statistical significance ($p = 0.0029$), confirming it as the most influential variable — higher temperatures within the range enhanced oil yield, consistent with improved solvent penetration and mass transfer. Extraction time and particle size were not significant as linear terms ($p = 0.2039$ and 0.6351, respectively), but this does not diminish their overall importance in the model.

Among the interaction terms, only the time–particle size interaction (BC) was statistically significant ($p = 0.0270$), with a negative coefficient (–3.63). This antagonistic interaction implies that the positive effect of one factor diminishes at higher levels of the other. All quadratic terms (A^2, B^2, and C^2) were highly significant (p-values of 0.0001, <0.0001, and 0.0048, respectively) and carried large negative coefficients (–9.78, –10.58, and –5.14). These negative quadratic effects produce a downward-opening parabolic response surface for each variable, clearly indicating the presence of an optimal point within the experimental range. Beyond these optima, further increases in temperature, time, or changes in particle size lead to reduced yields — likely due to thermal degradation of bioactive components or mass transfer limitations associated with very fine or coarse particles.

Finally, the variance inflation factors (VIF) for all terms were very low (1.00–1.01), confirming the absence of multicollinearity among the variables. This ensures that the estimated coefficients are stable and reliable for interpretation and prediction.

The regression analysis indicated that quadratic models provided the best fit, which can be represented in terms of coded factors by equation (3).

$$\text{Yield}(\%) = +43.76+4.11A-1.29B+0.4563C+0.3925AB-0.3275AC-3.63BC-9.78A^2-10.58\ B^2-5.14C^2 \quad (3)$$

Table 2. Experimental Design Parameters Vs Oil Yields (Actual and Predicted Values).

Run	A:Reaction temperature(^{O}C)	B:Reaction time(min)	C:Particle size(mm)	Yield(Actual) %	Yield (Predicted)%
1	80	50	0.14	32.82	32.82
2	65	50	0.17	43.45	43.76
3	65	50	0.17	41.22	43.76
4	50	40	0.17	21.7	20.98
5	80	50	0.2	34.52	33.08
6	65	50	0.17	47.62	43.76
7	50	50	0.2	25.52	25.52
8	65	50	0.17	46.18	43.76
9	80	40	0.17	27.69	28.41

Run	A:Reaction temperature(^{O}C)	B:Reaction time(min)	C:Particle size(mm)	Yield(Actual) %	Yield (Predicted)%
10	65	60	0.2	22.86	23.58
11	80	60	0.17	25.9	26.62
12	65	40	0.2	32.69	33.41
13	65	50	0.17	40.33	43.76
14	65	60	0.14	30.64	29.92
15	65	40	0.14	25.97	25.25
16	50	60	0.17	18.34	17.62
17	50	50	0.14	22.51	23.95

Table 3. ANOVA analysis for Quadratic model

Source	Sum of Squares	df	Mean Square	F-value	p-value	
Model	1291.99	9	143.55	21.21	0.0003	significant
A-Reaction temperature	134.97	1	134.97	19.94	0.0029	
B-Reaction time	13.29	1	13.29	1.96	0.2039	
C-Particle size	1.67	1	1.67	0.2460	0.6351	
AB	0.6162	1	0.6162	0.0910	0.7716	
AC	0.4290	1	0.4290	0.0634	0.8085	
BC	52.56	1	52.56	7.77	0.0270	
A^2	402.32	1	402.32	59.44	0.0001	
B^2	471.09	1	471.09	69.60	< 0.0001	
C^2	111.35	1	111.35	16.45	0.0048	
Residual	47.38	7	6.77			
Lack of Fit	8.31	3	2.77	0.2836	0.8357	not significant
Pure Error	39.07	4	9.77			
Cor Total	1339.37	16				
Std. Dev.	2.60		R^2	0.9646		
Mean	31.76		Adjusted R^2	0.9191		
C.V. %	8.19		Predicted R^2	0.8552		
			Adeq Precision	13.1013		

Table 4. Coefficients in terms of Coded factors and Coefficient of Determination

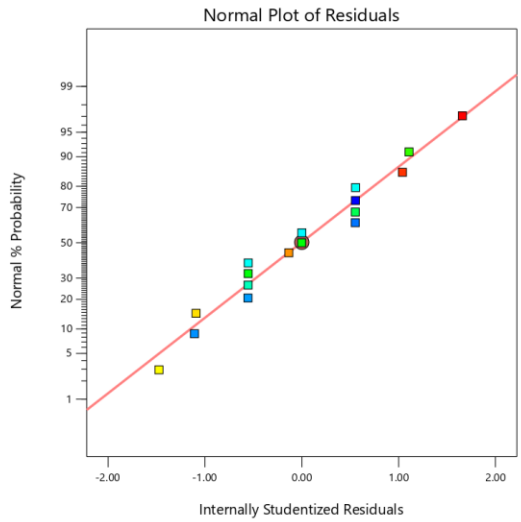
Factor	Coefficient Estimate	df	Standard Error	95% CI Low	95% CI High	VIF
Intercept	43.76	1	1.16	41.01	46.51	
A-Reaction temperature	4.11	1	0.9198	1.93	6.28	1.0000
B-Reaction time	-1.29	1	0.9198	-3.46	0.8862	1.0000
C-Particle size	0.4563	1	0.9198	-1.72	2.63	1.0000
AB	0.3925	1	1.30	-2.68	3.47	1.0000
AC	-0.3275	1	1.30	-3.40	2.75	1.0000
BC	-3.63	1	1.30	-6.70	-0.5491	1.0000
A^2	-9.78	1	1.27	-12.77	-6.78	1.01
B^2	-10.58	1	1.27	-13.58	-7.58	1.01
C^2	-5.14	1	1.27	-8.14	-2.14	1.01

Fig. 2 presents a normal probability plot of residuals, which assesses the assumption that the residuals differences between observed and model-predicted values follow a normal distribution. The close alignment of the data points along the theoretical diagonal line suggests no major deviations from normality. The absence of systematic curvature or points beyond the ±2.00 range further supports that the residuals are normally distributed, with no significant outliers detected.

Figure 3 illustrates the relationship between experimentally obtained response values and those predicted by the model. The strong clustering of data points near the 45-degree reference line indicates high predictive accuracy. This close agreement between observed and predicted values confirms the model's robustness and its capability to reliably estimate responses within the experimental domain according to the author Aseibichin *et al*, (2024).

The residual versus predicted plot as shown in Figure 4, shows the ideal pattern is a random scatter of points within a constant band around zero. In the provided plot, the residuals are scattered randomly above and below zero without forming any obvious patterns The variance appears consistent across all levels of the predicted response.

Figure 5 shows the order of the experimental runs should be random to avoid biases. The provided plot shows residuals randomly scattered within the control limits (±3.00) with no obvious upward or downward trend over time. There is no visible cyclical pattern or shift in the data.



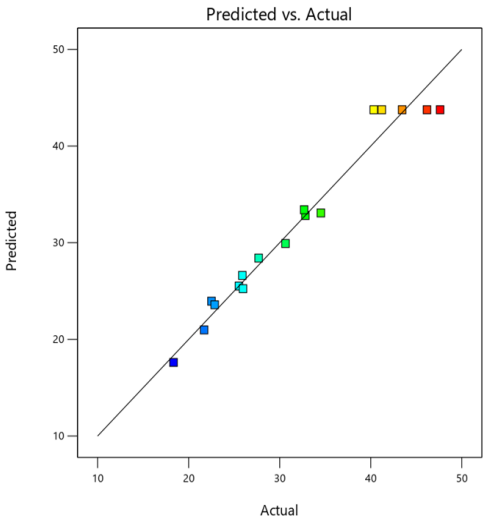
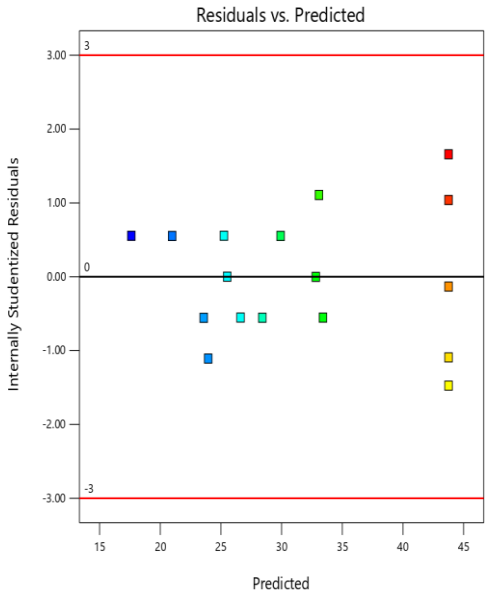


Figure 2(a). Normal Plot of Residuals (a)

Figure 2(b). Experimental yield Vs Predicted yield



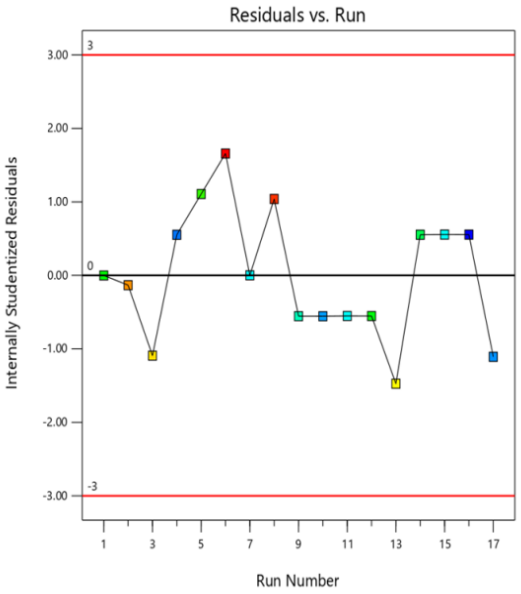


Figure 2 (c). Residual Vs Prediction,

Figure 2 (d). Residual Vs Number of the runs

Interactive Effects of Process Parameters on the Yield of Oil

Interactive Effects Reaction Temperature and Reaction Time

The 3D surface plot (Figure 3a) visualizes the quadratic relationship between yield (%) and the two factors. It shows a curved, hill-like (or saddle-shaped) response surface with a clear maximum in the central region. The highest yields (approaching ~45-50% based on the color scale and peak) occur at intermediate-to-higher temperatures (roughly 60-70°C) and moderate reaction times (around 45-55 min). The surface rises from lower values at the corners (e.g., low temperature/short time or extremes) and exhibits some curvature indicating interaction effects between temperature and time. Red spheres likely mark experimental design points (including center points and axial/corner combinations typical of BBD), highlighting the empirical data supporting the model (Madondo et al., 2022).

This curvature confirms that both linear and quadratic terms are significant, and an optimum exists within the studied domain rather than at the boundaries a key advantage of BBD/RSM for avoiding extreme conditions while efficiently mapping the response (Abdel et al., 2024).

The 2D contour plot (Figure 3b) (top-down projection) reinforces this with concentric elliptical/circular contours centered around ~62-68°C and ~50 min, where the yield is maximized (bright yellow/orange "hot spot"). The color gradient (blue/green → yellow → orange/red) clearly delineates regions of low to high yield. This plot is excellent for identifying the stationary point (optimum) and assessing sensitivity: small deviations from the center cause moderate yield drops, suggesting a relatively robust optimum (Halici et al., 2025)..

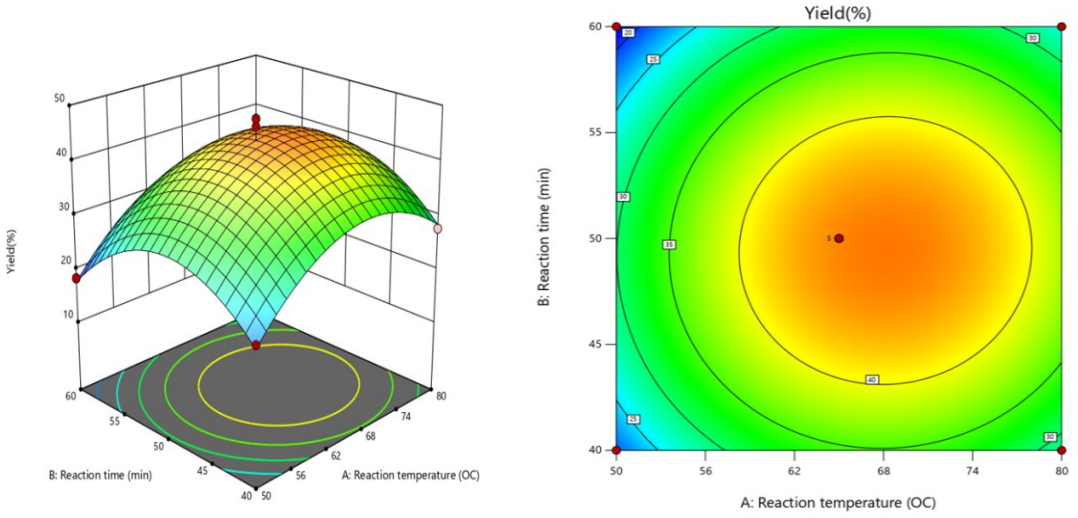


Figure 3. 3D Surface plots (a) and Contour plot (b) for interaction effect of reaction temperature and reaction time

Interactive Effects of Reaction Temperature and Particle Size

The 3D surface (Figure 4a), shows a curved (saddle/elliptical) response with a clear peak yield around mid-to-higher temperatures (65–75°C) and smaller particle sizes (0.14–0.17 mm). Yield drops sharply at lower temperatures and larger particles, indicating strong interactive effects. Red markers highlight experimental/optimal points (Ghasemi et al., 2024). The 2D contour (Figure 4b), reinforces this: a bright yellow-orange high-yield zone centered around ~68–74°C and 0.16–0.18 mm, with concentric ellipses showing the direction of steepest ascent/descent. Smaller particles increase surface area for better heat/mass transfer, while moderate temperature provides activation energy without degradation (Mariyam et al., 2024).

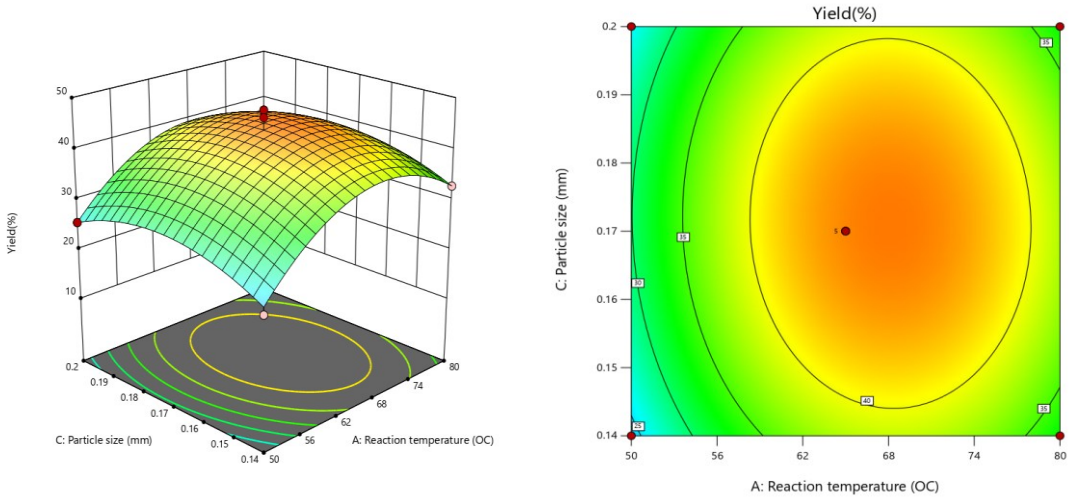


Figure 3. 3D Surface plots (a) and Contour plot (b) for interaction effect of reaction temperature and particle size

Interactive Effects Reaction Time and Particle Size

The 3D surface displays a pronounced peak near 50–55 min and smaller particle sizes (0.15–0.17 mm), with yield declining at extremes (very short/long times or larger particles). The surface is smoother than the temperature plot, suggesting time has a quadratic but slightly less dominant effect.

The 2D contour shows an elongated high-yield elliptical region (yellow-orange) around the center (50 min, 0.17 mm), confirming an optimal sweet spot. Longer times may allow equilibrium, but excessive time risks side reactions or product decomposition; smaller particles facilitate faster diffusion (Ayub et al., 2024).

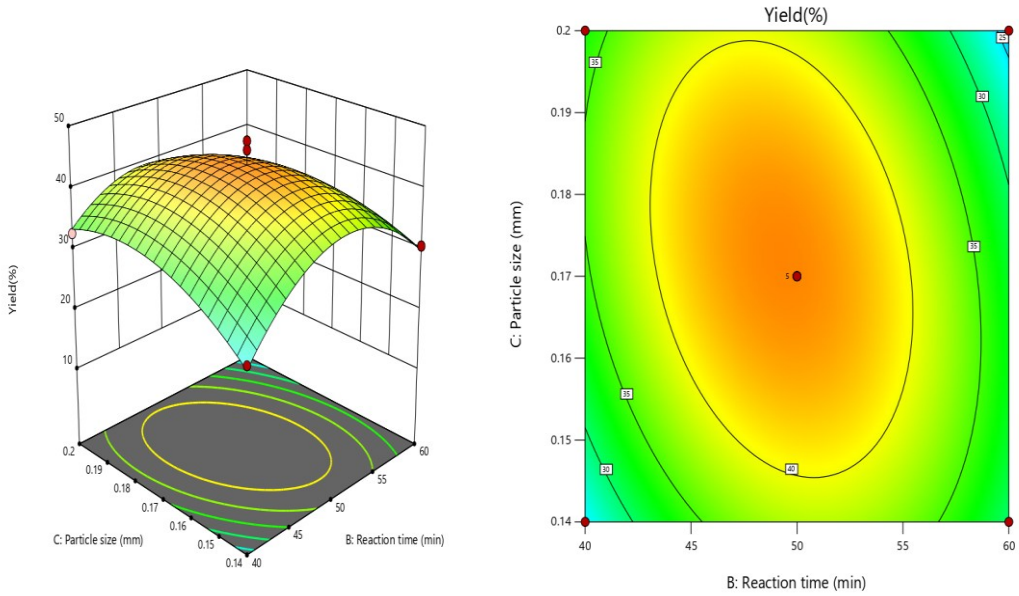


Figure 3. 3D Surface plots (a) and Contour plot (b) for interaction effect of reaction time and particle size

Numerical Optimization

Numerical optimization using Design-Expert software (maximizing oil yield) (Fig.4), identified the following optimal conditions: reaction temperature 66.55 °C (95% CI: 64.8–68.3 °C), extraction time 49.84 min (95% CI: 47.9–51.8 min), and particle size 0.144 mm (95% CI: 0.140–0.148 mm), with a predicted yield of 39.93% (95% Prediction Interval: 36.9–42.9%) and desirability of 1.000.

The 95% confidence intervals reflect the uncertainty in the location of the optimum, while the prediction interval incorporates both model uncertainty and inherent experimental variability. Validation experiments at these optimum conditions gave yields ranging from 39.5–40.4%, falling comfortably within the 95% prediction interval and confirming a low prediction error (<2.5%). This demonstrates the reliability and practical applicability of the developed quadratic model.

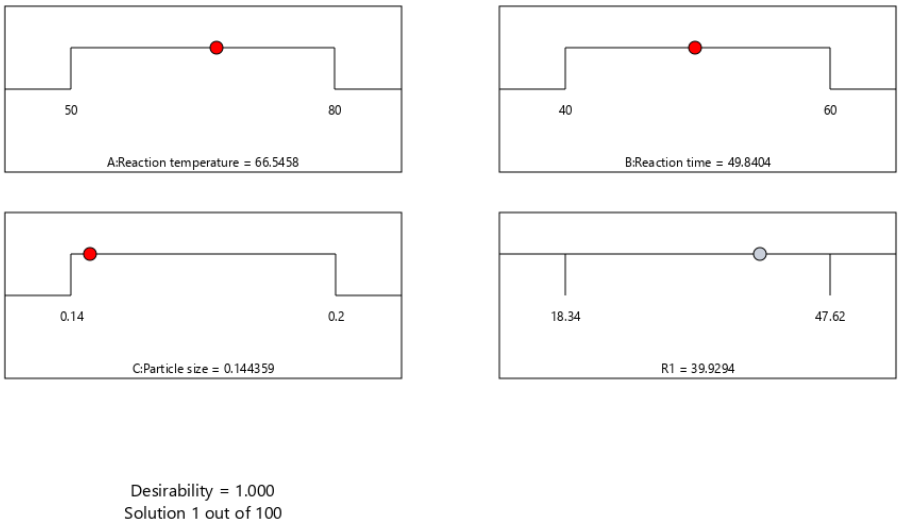


Figure 4: Ramps Plot (Numerical Optimization)

Effect of Extraction Temperature on Solvent Viscosity, Diffusion Coefficients, and Solubility of Triglycerides

In solvent extraction of neem seed oil (and other vegetable oils) using n-hexane in a Soxhlet apparatus, extraction temperature is a critical process parameter that influences mass transfer and yield through its effects on solvent properties and solute behavior.

Solvent Viscosity: Increasing temperature reduces the viscosity of n-hexane. Lower viscosity improves solvent penetration into the seed matrix and enhances flow through the porous structure of the ground seeds. This facilitates better contact between the solvent and the oil-containing cells (Bakhshabadi et al., 2025).

Diffusion Coefficients: Higher temperatures increase the diffusion coefficient of triglycerides within the solvent and plant matrix. According to the Arrhenius relationship, elevated temperature imparts greater kinetic energy to molecules, reducing intermolecular forces and accelerating diffusion. This leads to faster mass transfer of oil from the interior of seed particles to the bulk solvent, particularly important in the diffusion-controlled phase of Soxhlet extraction (Mkhize et al., 2023).

Solubility of Triglycerides: Temperature positively affects the solubility of triglycerides in n-hexane. Higher temperatures disrupt cohesive forces between oil molecules and the seed matrix while increasing the solvating power of the solvent, resulting in higher equilibrium solubility and improved extraction yields. However, the temperature must be controlled to avoid degradation of thermolabile bioactive compounds (Mustapha et al., 2024).

Analysis of Properties of Neem Seed Oil

Specific gravity (0.89) and Density (0.88 g/cm³): These values fall within the typical range for many vegetable oils (0.87–0.92). They indicate a relatively light oil suitable for liquid fuel applications after processing (Sudalai et al., 2025). Moisture content (4.61%): Moderately high. Excess moisture can promote hydrolysis, increase free fatty acids (FFA), and reduce biodiesel yield. Pre-drying is usually recommended.

Ash content (2.1%): Elevated compared to refined oils (<0.1–0.5%). This suggests potential mineral impurities or contamination, which may affect catalyst performance or cause engine deposits in the final fuel. Kinematic viscosity (32.2 mm²/s): Very high (typical for crude vegetable oils: 25–40 mm²/s). This is far above biodiesel standards (1.9–6.0 mm²/s), confirming the need for transesterification to reduce viscosity (Hájek et al., 2021) . Saponification value (202 mg KOH/g) : Indicates average molecular weight of fatty acids. Values around 190–210 are common for oils rich in C16–C18 fatty acids and suggest good potential for soap or biodiesel production (Hatsa et al., 2025). Iodine value (118.5 g I_2/100g): Reflects a moderate-to-high degree of unsaturation (likely high linoleic/oleic content). This supports good cold-flow properties but may imply moderate oxidative stability. EN 14214 limit is ≤120 . Acid value (172 mg KOH/g): Extremely high (corresponding to very high FFA content, ~86% as oleic acid). This classifies the oil as a high-FFA feedstock, requiring acid-catalyzed esterification pre-treatment before base-catalyzed transesterification to avoid soap formation.

Table 5. Physiochemical Properties of Neem Seed Oil

Parameters	Value
specific gravity	0.89
Density	0.88
moisture content	4.61
Ash content	2.1
Kinematic viscosity	32.2
Saponification value	202
Iodine value	118.5
Acid value	172

Fourier Transform Infrared Spectroscopy (FTIR) Functional Group Analysis

The spectrum of neem oil in Fig. 7 provides a unique fingerprint that confirms the presence of major lipid components and bioactive compounds. A broad, strong peak in this region 3200-3600 cm^{-1} (O-H Stretching Vibrations) is primarily indicative of hydroperoxides, which are primary oxidation products. It can also signify the presence of free fatty acids, alcohols, or moisture. The intensity of this peak can be a marker for the oil's oxidative stability and freshness; a more pronounced peak suggests a higher degree of oxidation. Two strong

peaks:2925 cm^{-1} and 2854 cm^{-1} shows asymmetric stretching of CH_2 groups (methylene groups in fatty acid chains) by the authors Kumar and Sharma, (2024).

A smaller shoulder at peak 3008 cm^{-1} is characteristic of =C-H stretching vibration of cis-double bonds, confirming the presence of unsaturated fatty acids like oleic acid.

A very strong, sharp peak in this region is the most characteristic feature of triglycerides. It represents the ester carbonyl group (C=O) stretching vibration from the glycerol backbone of the oil. This peak is a definitive indicator of the oil nature. At peak 1465 cm^{-1} indicates scissoring bending vibration of CH_2 groups. At peak 1377 cm^{-1}: Symmetric bending vibration of terminal CH_3 groups. These peaks further confirm the presence of the aliphatic hydrocarbon chains. A strong, complex band in this region is due to the C-O stretching vibrations of the ester functional group (O-C-C) in triglycerides. This is a key peak that, along with the C=O peak, confirms the triester structure of the oil. A small but distinct peak near 720 cm^{-1} indicates rocking vibrations of methylene (CH_2) groups in long-chain fatty acids with four or more methylene groups [$(CH_2)_n$, where $n \geq 4$]. It is common in most vegetable oils.

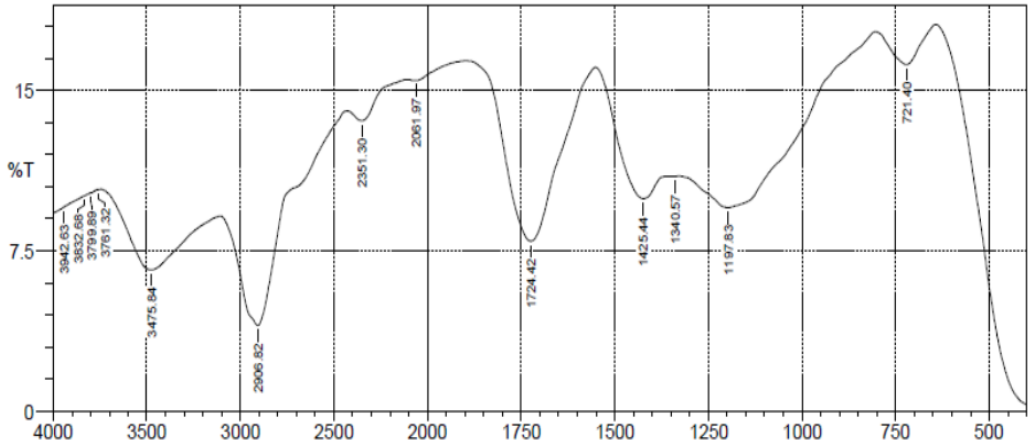


Figure 7. FITR of Extracted Neem Oil

Conclusion

This study successfully optimized the solvent extraction of neem seed oil using a Box-Behnken Design under Response Surface Methodology. The quadratic model adequately described the relationship between the process variables (temperature, time, and particle size) and oil yield, as evidenced by high R^2 (0.9646), non-significant lack of fit, and strong agreement between experimental and predicted values. Temperature and the quadratic terms of all factors exerted the most significant effects on yield. The optimal conditions produced a high desirability solution with a predicted yield of approximately 42.9%, consistent with the response surface plots. Physicochemical characterization of the extracted oil revealed typical vegetable oil properties, albeit with a notably high acid value (172 mg KOH/g), high viscosity,

and moderate unsaturation, confirming its potential as a promising non-edible biodiesel feedstock after appropriate pre-treatment. FTIR spectroscopy further validated the triglyceride-rich composition of the oil. Overall, this work demonstrates the effectiveness of RSM-BBD in enhancing extraction efficiency while contributing to the sustainable utilization of neem seeds.

Recommendation / Future Perspective

It is recommended that the optimized conditions (67.85 °C, 49.17 min, and 0.187 mm particle size) be validated through confirmatory experimental runs at laboratory and pilot scales to confirm the predicted yield. Further studies should focus on the two-step conversion of this high-FFA neem oil into biodiesel (acid esterification followed by alkaline transesterification) and comprehensive evaluation of the resulting biodiesel against ASTM D6751 and EN 14214 standards.

Future perspectives include scaling up the optimized extraction process, exploring greener solvents or ultrasound/microwave-assisted extraction to reduce extraction time and solvent consumption, and investigating the recovery of bioactive limonoids (e.g., azadirachtin) alongside oil extraction for higher-value applications in biopesticides and pharmaceuticals. Techno-economic and life-cycle assessments would also be valuable for industrial implementation. Additionally, genetic improvement of neem varieties for higher oil content and lower FFA levels could enhance overall process viability.

References

Abdel Hamid, E. M., Amer, A. M., & Mahmoud, A. K. (2024). Box-Behnken design (BBD) for optimization and simulation of biolubricant production from biomass using Aspen Plus with techno-economic analysis. Scientific Reports, 14, Article 21769. https://doi.org/10.1038/s41598-024-71266-w

Ameen, M., Zafar, M., Ahmad, M., Munir, M., Abid, I., Mustafa, A. E.-Z. M. A., Athar, M., Makhkamov, T., Mamarakhimov, O., Yuldashev, A., Khaydarov, K., Mammadova, A. O., Botirova, L., & Makkamov, Z. (2023). Cleaner biofuel production via process parametric optimization of nonedible feedstock in a membrane reactor using a titania-based heterogeneous nanocatalyst: An aid to sustainable energy development. Membranes, 13(12), Article 889. https://doi.org/10.3390/membranes13120889

Amin, M. M., Nallamothu, R. B., Ancha, V. R., & Alemayehu, G. (2026). Extraction, process optimization, and characterization of Aloe weloensis oil (AWO) using Box–Behnken design (BBD) and FTIR analysis. Journal of Engineering, 2026, Article 8880521. https://doi.org/10.1155/je/8880521

Aseibichin, C., Ulakpa, W. C., Omenogor, I., Doyah, E., Olaseinde, A. A., Anakpoha, O. C., Keke, M., & Karuppannan, S. (2024). Modeling and optimization of transesterification of Jatropha oil to fatty acid methyl ester: Application of response surface methodology (CCD) and Taguchi orthogonal method. RSC Advances, 14, 11784–11796. https://doi.org/10.1039/d4ra01149j

Ayub, M. A., Iram, I., & Waseem, R. (2024). Optimizing the extraction of essential oil yield from Pistacia lentiscus oleo-gum resin by superheated steam extraction using response surface methodology. Scientific Reports, 14, Article 25769. https://doi.org/10.1038/s41598-024-74972-7

Bakhshabadi, H., Ganje, M., Gharekhani, M., Mohammadi-Moghaddam, T., Aulestia, C., & Morshedi, A. (2025). A review of new methods for extracting oil from plants to enhance the efficiency and physicochemical properties of the extracted oils. Processes, 13(4), Article 1124. https://doi.org/10.3390/pr13041124

Ghasemi, G., Fattahi, M., & Alirezalu, A. (2024). Screening genotypes and optimizing ultrasonic extraction of phenolic antioxidants from Rheum ribes using response surface methodology. Scientific Reports, 14, Article 21544. https://doi.org/10.1038/s41598-024-72214-4

Halici, Z., & Demirhan, E. (2025). Response surface methodology for optimizing adsorption process parameters for tadalafil removal by raw eggshell. Biomass Conversion and Biorefinery, 15, 6027–6036. https://doi.org/10.1007/s13399-024-05380-0

Hájek, M., Vávra, A., de Paz Carmona, H., & Kocík, J. (2021). The catalysed transformation of vegetable oils or animal fats to biofuels and bio-lubricants: A review. Catalysts, 11(9), Article 1118. https://doi.org/10.3390/catal11091118

Hatsa, T. M., Kelile, A. W., & Beyene, E. G. (2025). Production and comprehensive analysis of biodiesel from Dovyalis caffra seed oil. Sustainable Energy Research, 12, Article 17. https://doi.org/10.1186/s40807-025-00161-3

Kazam, J., Iqbal, K. J., Shafi, A., Majeed, U., & Lackner, M. (2025). Neem oil (Azadirachta indica L.) response surface methodology (RSM)-optimized nanoemulsions for sensory quality preservation of Oreochromis niloticus fillets. Biology, 14(4), Article 400. https://doi.org/10.3390/biology14040400

Madondo, N. I., Rathilal, S., & Bakare, B. F. (2022). Utilization of response surface methodology in optimization and modelling of a microbial electrolysis cell for wastewater treatment using Box–Behnken design method. Catalysts, 12(9), Article 1052. https://doi.org/10.3390/catal12091052

Mariyam, S., Alherbawi, M., & Pradhan, S. (2024). Biochar yield prediction using response surface methodology: Effect of fixed carbon and pyrolysis operating conditions. Biomass Conversion and Biorefinery, 14, 28879–28892. https://doi.org/10.1007/s13399-023-03825-6

Martínez-Castro, R., Flórez-Santiago, J., Valle-Molinares, R., Cabrera-Barraza, J., & Espitia-Almeida, F. (2024). Optimized microwave-assisted azadirachtin extraction using response surface methodology. Heliyon, 10(10), Article e31504. https://doi.org/10.1016/j.heliyon.2024.e31504

Mkhize, Z. I., Ngema, P. T., & Ramsuroop, S. (2023). Effect of temperature on extraction of castor oil from castor seeds using potential green solvents. Advances in Chemical Engineering and Science, 13, 301–317. https://doi.org/10.4236/aces.2023.134021

Mustapha, S., Habib, M. U., Ma'aruf, A. M., Mustapha, A., & Shehu, H. (2024). Sustainable technique for neem (Azadirachta indica) seed oil extraction: Optimization and characterization. African Journal of Environment and Natural Science Research, 7(2), 218–228. https://doi.org/10.52589/AJENSR-5H1FVLHR

Nde, D. B., & Foncha, A. C. (2020). Optimization methods for the extraction of vegetable oils: A review. Processes, 8(2), Article 209. https://doi.org/10.3390/pr8020209

Sudalai, S., Varalakksmi, V., & Rahul, S. (2025). Sustainable biodiesel production from Ceiba pentandra (Kapok): A scientometric and technological assessment with performance, emission insights, and future challenges. Biotechnology for Biofuels and Bioproducts, 18, Article 121. https://doi.org/10.1186/s13068-025-02710-w

Suttiarporn, P., & Choommongkol, V. (2020). Microwave-assisted improved extraction and purification of anticancer nimbolide from Azadirachta indica (Neem) leaves. Molecules, 25(12), Article 2913. https://doi.org/10.3390/molecules25122913

Wisdom, C. U., Ulakpa, R. O. E., Eyankware, E. O., & Egwunyenga, M. C. (2022). Statistical optimization of biodiesel synthesis from waste cooking oil using NaOH/bentonite impregnated catalyst. Cleaner Waste Systems, 3, Article 100049. https://doi.org/10.1016/j.clwas.2022.100049